ELSEVIER

Contents lists available at ScienceDirect

Biosensors and Bioelectronics

journal homepage: www.elsevier.com/locate/bios



In situ plasmonic generation in functional ionic-gold-nanogel scaffold for rapid quantitative bio-sensing



Santosh K. Misra a,b,1 , Ketan Dighe a,b,1 , Aaron S. Schwartz-Duval a,b,1 , Zaixi Shang a,b , Leanne T. Labriola d,e,f , Dipanjan Pan a,b,c,f,*

- a Department of Bioengineering, Materials Science and Engineering, Beckman Institute, University of Illinois Urbana-Champaign, Urbana, IL, USA
- ^b Mills Breast Cancer Institute, Carle Foundation Hospital, Urbana, IL, USA
- ^c Carle Illinois College of Medicine, Urbana, IL, USA
- ^d Ophthalmology Department, Carle Foundation Hospital, Urbana, IL, USA
- ^e Surgery Department, University of Illinois College of Medicine, Urbana, IL, USA
- f Interdisciplinary Health Science Initiative, University of Illinois, Urbana, IL, USA

ARTICLE INFO

Keywords: Plasmonic nanogel Gold nanoparticles Biosensors Ascorbic acid Tear film Biomarker Point-of-care (POC)

ABSTRACT

Conventional analytical techniques, which have been developed for high sensitivity and selectivity for the detection and quantification of relevant biomarkers, may not be as suitable for medical diagnosis in resource scarce environments as compared to point-of-care devices (POC). We have developed a new reactive sensing material which contains ionic gold entrapped within an agarose gel scaffold for POC quantification of ascorbic acid (AA) in tear fluid. Pathologically elevated concentration of AA in human tear fluid can serve as a biomarker for full-thickness injuries to the ocular surface, which are a medical emergency. This reactive sensing material will undergo colorimetric changes, quantitatively dependent on endogenous bio-reductants that are applied, as the entrapped ionic gold is reduced to form plasmonic nanoparticles. The capacity for this reactive material to function as a plasmonically driven biosensor, called 'OjoGel' (ojo-eye), was demonstrated with the endogenous reducing agent, AA. Through applications of AA of varied concentrations to the OjoGel, we demonstrated a quantitative colorimetric relationship between red (R) hexadecimal values and concentrations of AA in said treatments. This colorimetric relationship is directly resultant of plasmonic gold nanoparticle formation within the OjoGel scaffold. Using a commercially available mobile phone-based Pixel Picker application, the OjoGel plasmonic sensing platform opens a new avenue for easy-to-use, rapid, and quantitative biosensing with low cost and accurate results.

1. Introduction

Conventional laboratory based analytical methods, at hospitals and clinics, which are used to diagnose pathologies through biomarker detection and estimation are highly sensitive and selective (Deng et al., 2014; Jans and Huo, 2012; Song et al., 2010; Wang et al., 2014; Whitcombe et al., 2011) (such as ELISA (Fredriksson et al., 2002; Manenschijn et al., 2011), ECLIA (Carrozza et al., 2010), electrochemical analyses (Nie et al., 2009), HPLC (Klopfenstein et al., 2011), fluorometric assay, RIA (Kaushik et al., 2013), and PAGE (Vallejo-Illarramendi et al., 2013)). While these laboratory based analytical techniques are excellent in terms of sensitivity and selectivity, they are costly, time intensive, require highly trained staffers, and can only be utilized in the lab-based hospital where the large stationary-equipment,

isotopes, and reagents can be accessed in order to perform said analytical techniques. These restrictions become major hurdles for situations with resource scarcity. To address this issue, resources have been aimed toward the development of POC testing; which are tests that can be used directly on the patient during the examination to provide an immediate result (Kattumuri et al., 2006; Luppa et al., 2012). These POC testing devices enable more frequent testing, allow earlier pathological detection, as well as potentially giving patients a heightened sense of self-control and ownership of their own healthcare. Of these POC testing devices, there has been much success utilizing solution-based plasmonic nanoparticle colloids as colorimetric sensors for biological analytes (Sotiriou et al., 2010). The potential of Surface Plasmon Resonance (SPR) biosensing has received enormous interest since its first application (Evanoff and Chumanov, 2005). These SPR sensing

^{*} Corresponding author.

E-mail address: dipanjan@illinois.edu (D. Pan).

¹ Authors have contributed equally to this work.

strategies typically rely on plasmonic sensor-bound biomolecules, which specifically bind to target analytes (Evanoff and Chumanov, 2005; Sotiriou et al., 2010). When the analyte selectively binds to its specific plasmonic sensor-bound biomolecule this enables analyte detection through a local change in refractive index (Evanoff and Chumanov, 2005; Sotiriou et al., 2010). Protein biomolecules which have a higher refractive index than aqueous solutions cause a red shift in plasmonic absorption spectra which can be used for label-free biosensing (Sannomiya et al., 2008; Willets and Van Duyne, 2007). SPR as such has been used in many actual and potential applications including electronic devices (Schuller et al., 2010), biosensing (Tian and Tatsuma, 2005), catalysis (Tian and Tatsuma, 2005), and photochemistry (Uechi and Yamada, 2008). Moreover, SPR based biosensors have been proven to show excellent applications in the field of biotechnology, biochemistry, bioengineering, biomolecular interaction, chemical detection, medical diagnostics and immunoassays as diagnostic probes for infectious diseases, ion sensing, protein-DNA interactions, binding events and biological surface modifications (Campbell and Kim, 2007; Eum et al., 2003; Jeong et al., 2008; Lee et al., 2015; Patskovsky et al., 2008; Shankaran et al., 2007; Vo-Dinh and Cullum, 2000; Yeom et al., 2013). Most of the plasmonic based biosensors use gold (Au) as plasmonic material as the element supports plasmon resonance in the middle of visible region, exhibit excellent resistance to oxidation, non-toxic and readily fabricated into nanostructures (Qiu et al., 2018; Takemura et al., 2017; Schwartz-Duval, 2016). Herein, we have developed a new reactive sensing material, called 'OjoGel', composed of ionic gold interspersed through agarose gel scaffolding. Our hypothesis is that upon interaction with reductive molecules the OjoGel will undergo colorimetric changes through plasmonic nanoparticle formation in a quantifiable manner dependent on the concentration of the reductant molecules. To test the application of the OjoGel, we utilized ascorbic acid (AA) as a potential endogenous reductant due to its reductive capacity $(E^0 = +0.06 \text{ V}, 25 ^{\circ}\text{C})$ (Matsui et al., 2015). The concentration of AA within the external ocular tear film (TF) (23 \pm 9.6 μ mol/L) is magnitudes lower than AA concentration within internal aqueous humor (AH) (1049 \pm 433 μ mol/L), and as such, pathologically elevated levels of AA within the TF that result from a direct leak of AH into the tear fluid can serve as a surrogate biomarker of anterior scleral or corneal wound integrity (Ajit and Pandya, 2014; Choy et al., 2000; Leite et al., 2009; Taylor et al., 1995). The AH is a clear, water-like, low-protein containing fluid that is secreted from the ciliary epithelium. AH is continuously produced within the anterior chamber of the globe (Grüb and Mielke, 2004; Millar et al., 2018), therefore, if the integrity of the anterior globe is disturbed, the concentration of AA in the TF will rise due to direct contamination of the tear fluid with AH. These variations of endogenous reductant concentrations between intact TF and AH (as AA) demonstrate one of many potential utilities for our OjoGel biosensor. We have characterized a quantifiable colorimetric relationship between OjoGel treatments of AA (in solutions of varied complexity) and resulting Red-Green-Blue (RGB) values acquired from mobile phone images (with Pixel Picker® application). In demonstrating the capacity of the OjoGel to determine AA concentration in de-ionized water (DI-H2O), contrived tear film (CTF), and clinical samples of AH, we have confirmed that the OjoGel can be utilized to detect ocular integrity through measuring the variations in AA concentration of patient TF samples. This increased level of AA could be tested using OjoGel tubes and concentrations determined using simple Pixel Picker mobile phone application.

2. Experimental

2.1. Synthesis of OjoGel

The gold(III) chloride-agarose gel (2% OjoGel) was developed by dissolving 23.1 mg of gold(III) chloride hydrate 99.99% salt in 2.271 ml of DI-H $_2$ O to obtain a final concentration of 30 mM. Then 1 ml of 30 mM

gold(III) chloride solution was mixed with 160 mg of agarose powder in 4 ml of DI- $\rm H_2O$ in a 20 ml disposable scintillation vial. The total solution of 5 ml was then heated in a microwave for 90 s. The hot solution was immediately transferred into centrifuged tubes and a capillary tube was placed to create a small channel in the middle of the gel. The solution was allowed to solidify at room temperature (RT) for around 30 min and was later stored at 4 $^{\circ}$ C until further use (Fig. 2A).

2.2. Ascorbic acid detection using commercial ELISA kit

The ELISA experiments were performed using a 96-well plate. Six known concentrations (0, 2, 4, 6, 8, 10 nmol) per Liter of AA and five human AH samples (1–5) with unknown AA concentration were pipetted into the microliter plate wells with a volume of 120 μL (AA/AH Sample Plus AA Assay Buffer) of each sample. 30 μL of catalyst was then added to each standard and sample well. After 15 min incubation at RT (18–25 °C), 50 μL of the reaction mix was added to each well containing the AA Standard and test samples. A color (pink) is developed within 3 min and stable for an hour. After 30 min, each well was then measured for 2 s in a Spectrophotometer with Gen 5.0 software at 490 nm OD. Measurements were tested in duplicate sets, and the average value was then utilized to determine the final AA concentration.

2.3. Quantification of gold(III) chloride reduction and correlation to ascorbic acid concentration

In order to find out the reducing activity of AA on gold(III) chloride solution to form gold nanoparticles we conducted a series of trials in which we took pictures with a normal cellphone. At first, we made standard AA solution with concentrations of 2000 µM, 1000 µM, $500\,\mu\text{M},\,250\,\mu\text{M},\,125\,\mu\text{M},$ and $50\,\mu\text{M}.$ The standards are then delivered to the channel created in the gel with help of another capillary glass tube to get some color change which is indicative of reducing activity of AA on gold(III) chloride solution. The gels showed different color changes when reacted with samples of different concentrations. To establish a scale, we put the reacted PCR tubes together in a PCR stand. A number of pictures (50) were taken for each concentration from one side with the varying distance of a flash light. An app (Pixel Picker® available on Apple App Store™) was used to figure out the RGB value in the color changed areas. We did the same statistics for 50 pictures and found the average of the RGB values for each color changed area. Then we restore a color sequence based on the calculated RGB average and correlate it with the standard concentration of AA. Based on this optimized information, a color code ring was developed with assigned shade of color representing a nominal gold reduction and related AA concentration. OjoGel tubes were placed in these color rings before capturing snaps of changed color in OjoGel tubes. Color changes were co-related with used AA concentration.

2.4. Extraction of nanoparticles from OjoGel via sodium hypochlorite based dissolving method

Identified portions of reacted OjoGel were first removed via stainless steel spatula and placed into 1.5 ml microcentrifuge tubes. To the microcentrifuge tubes containing reacted OjoGel 1 ml of 15% w/v sodium hypochlorite solution admixed, sealed, and incubated for 45 min at 65 °C to dissolve the gel. The dissolved gel (65 °C) was then diluted 1:100 fold in room temperature DI-H $_2$ O before Raman spectroscopy or TEM measurements.

3. Results and discussion

3.1. Feasibility of plasmonic gold nanoparticle formation by free ascorbic acid and ascorbic acid in aqueous humor

Aqueous humor contains a wide variety of surfactants as well as

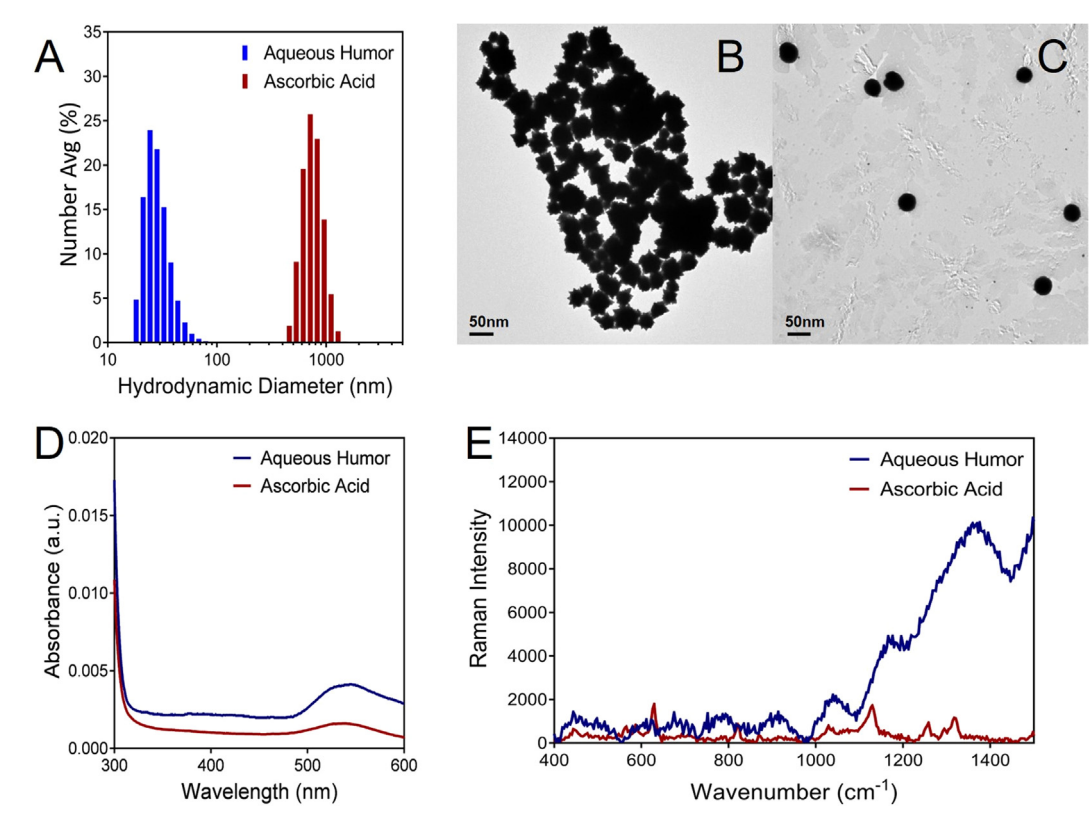


Fig. 1. (A) Hydrodynamic diameter of gold nanoparticles reduced with aqueous humor (blue) and ascorbic acid (red) 250 μ M. (B) TEM of gold nanoparticles reduced with ascorbic acid (50 nm scale bar) 250 μ M. (C) TEM of gold nanoparticles reduced with aqueous humor (50 nm scale bar). (D) UV–vis spectra of gold nanoparticles reduced with aqueous humor (blue) and ascorbic acid (red) 250 μ M. (E) Raman spectra of gold nanoparticles reduced with aqueous humor (blue) and ascorbic acid (red) 250 μ M.

containing high concentrations of AA, which can reduce gold(III) as an endogenous reductant to produce gold nanoparticles (Qin et al., 2010). In order to determine the feasibility of designing a plasmonic sensorbased detection of diffuse AA content in controlled solutions (containing only AA and water) with and more complex clinical samples required an initial screening. To determine this feasibility, we admixed ionic gold (Au3+) with either clinically acquired AH or AA at a concentration of 1 mM dissolved in DI-H2O. From these two mixed solutions, we observed colorimetric reactions occur; as the solution containing AH went from yellow to red with UV-vis absorbance peak at ~ 540 nm (characteristic of gold nanoparticles), and from yellow to clear (with visible brown aggregates) with an absorbance spectra identical with pure water from the solution with isolated AA (Fig. 1D). Through dynamic light scattering, we found that the mixture with isolated AA resulted in entities of sizes much larger (> 500 nm) than those produced with AH (~ 40 nm) (Fig. 1A). However, by utilizing transmission electron microscopy (TEM) we found that these larger entities were aggregations of nanoparticles ~ 40 nm in diameter (Fig. 1B). From this information, we can conclude that AA alone is sufficient to reduce the ionic gold but not to stabilize the nanoparticles enough to keep them segregated. AH, containing both reductant and stabilizing molecules resulted in colloidally stable nanoparticles (~ 30 nm anhydrous diameter through TEM) without aggregation (Fig. 1C). These results, indicating that gold nanoparticle reduction occurs via AA in pure solution and as component of AH, were further corroborated via surface enhanced Raman spectroscopy. To collect enhanced Raman spectra, mixed solutions of ionic gold with AA in pure solution and as component of AH were pipetted up and down to mix before being pipetted onto glass slides. Solutions on these slides were dried for > 24 h before Raman measurements were collected using a 635 nm laser. For the mixture containing only AA and ionic gold we see enhancement of AA signature without interference from other components (Fig. 1E) (De

Gelder et al., 2007). This enhancement found in the samples containing only AA and ionic gold is due to the nano-scaled features of the nanoparticle aggregates acting as "nano-antennae" (Schwartz-Duval et al., 2016; Yuan et al., 2012). If we compare this spectra with the mixture containing AH, we are able to observe much greater signal noise, as well as increase in overall Raman signal. This increase in intensity of Raman signal is causal of there existing a larger population of nanoparticles whose plasmonic absorbance matches the Raman laser wavelength. The Raman signal noise is due to the increased complexity of the mixture resulting from multiple molecules (not just AA) receiving plasmonically enabled Raman signal enhancement. Additionally, AA saturation concentration of gold chloride reduction was achieved by performing a UV-vis experiment where different titrated amounts of AA $(2 \mu M, 20 \mu M, 100 \mu M, 200 \mu M, 500 \mu M, 1000 \mu M$ and 2000 $\mu M)$ were used to reduce 3 mM of gold chloride solution. We observed that the intensity of plasmonic peak at 540 nm increased with increase in concentration of AA (Fig. S1). The peak intensity was found to be saturated at $1000\,\mu\text{M}$. This indicates that $1000\,\mu\text{M}$ of AA is enough to reduce 3 mM gold(III) chloride solution. This led to use of 30 mM gold chloride solution in preparation of OjoGel for providing a wider range of AA in standard and patient samples. These findings, support the notion that bodily fluids containing endogenous reductants (such as AA) that can reduce ionic gold, forming plasmonic gold nanoparticles, could potentially be measured in quantifiable manner through optical colorimetric

3.2. Synthesis of OjoGel and detection of ascorbic acid via optical differentiation

It was established that gold chloride could be reduced with ophthalmic fluids known to contain high AA concentration and AA alone, however, AA was not effective in producing colloidally stable gold

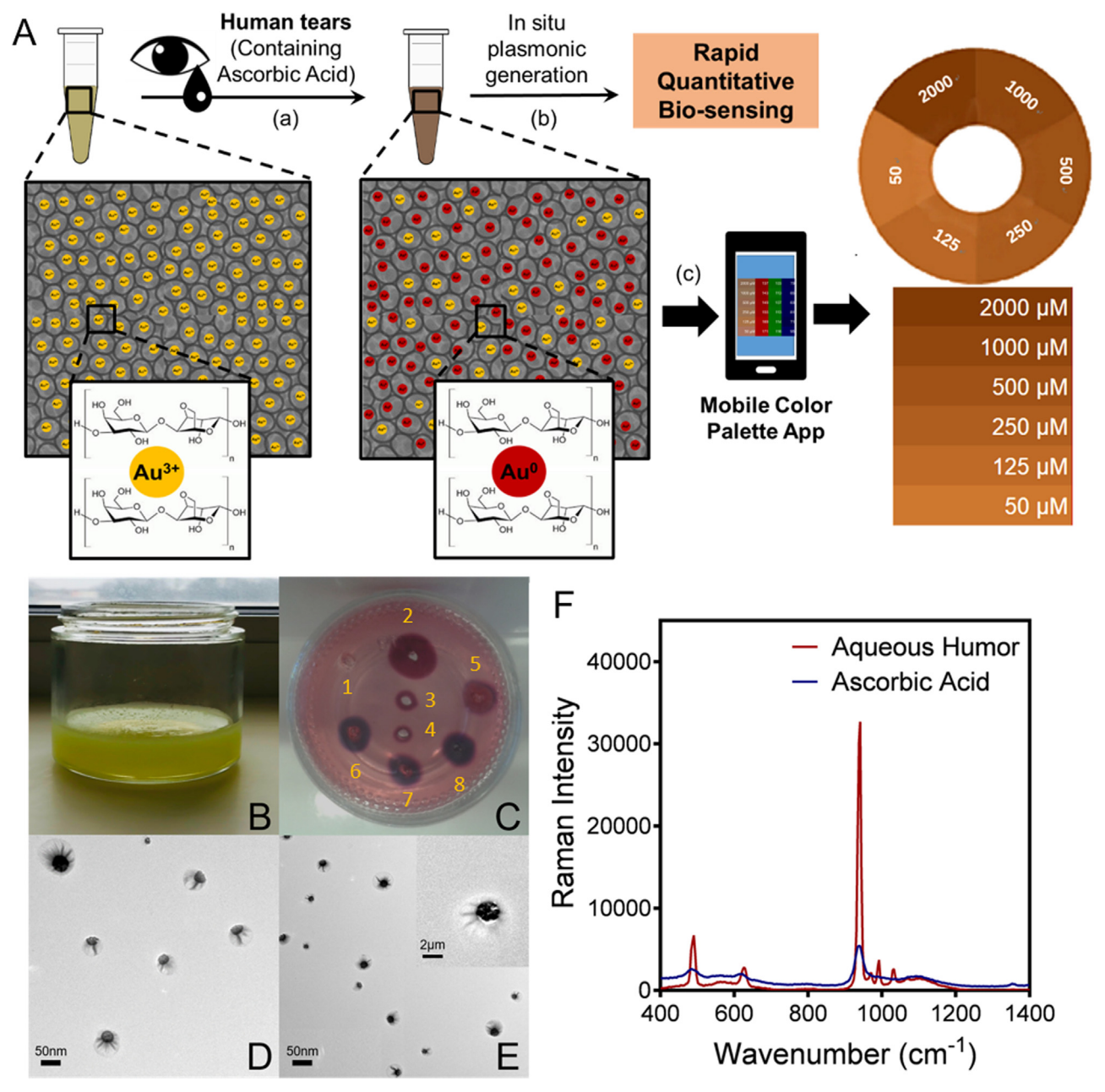


Fig. 2. (A) A schematic describing the correlation of color codes with AA concentration from OjoGels reduced with different tear film samples. Characterization of prepared OjoGel (B) before and (C) after reduction with AA concentrations. TEM images from reduced OjoGel obtained from (D) AA (1 mM; Spot 2). Inset represents calculated Feret diameter of the jelly fish structure and (E) AH incubation (AH1; Spot 4). Inset represents TEM image of one unit of reduced gold as a jelly fish morphology. (F) Raman scattering pattern of reduced OjoGel with high signature intensity by AH.

nanoparticles without stabilizing agents. To address the issue of nanoparticle aggregation in technical grade standards (solutions free of nonanalyte biomolecules which are necessary for calibrations) we embedded ionic gold within an agarose gel scaffold, termed 'OjoGel,' as a plasmonic sensing platform where AA (or any other endogenous biological reductant) could be optically quantified (Fig. 2A).

To prepare the OjoGel, 1 ml of $30\,\text{mM}$ gold(III) chloride solution was admixed with 4 ml of 1.25% (w/v) agarose in DI-H₂O. The mixtures were microwaved for $90\,\text{s}$ (high power setting, using a conventional Sunbeam microwave), until solution was homogenous with care to ensure that the ionic gold not be microwaved for too long (causing auto-reduction). As the mixture became homogenous, it was poured and cast in $0.6\,\text{ml}$ centrifuge tubes for convenience (however the OjoGel can be cast into any number of shapes/ forms). Once cooled and solidified, the cast OjoGels were stored at $4\,^{\circ}\text{C}$ prior to experimental

measurement (Fig. 2A). To activate the OjoGel as a sensor for biologically endogenous reductants (AA), treatments were applied through channels made with glass capillary tubes. Upon treatment of OjoGel with AA or AH containing AA, the color of the gel would change to a mahogany/orange-brown due to an increased localized nanoparticle formation at the treatment site (Fig. 2A) and could be correlated with color codes (Fig. 2A). OjoGel sample (Fig. 2B) was incubated (5–30 min) with different AA and AH samples generating gold nanoparticles and related plasmonic color (Fig. 2C). Here spot 1–8 represent various volume and concentrations of AA in standard solution as spot 1 for 0 mM (5 μ L), spot 2 for 1 mM (5 μ L), spot 3 for 10 mM (5 μ L) and spot 4 for 100 mM (20 μ L) while AA in different AH samples (20 μ L) as spot 5 for AH1, Spot 6 for AH2, Spot 7 for AH3 and Spot 8 for AH4. This plasmonic nanoparticle formation resultant of treatment was confirmed through TEM images of nanoparticles extracted from OjoGel spots from

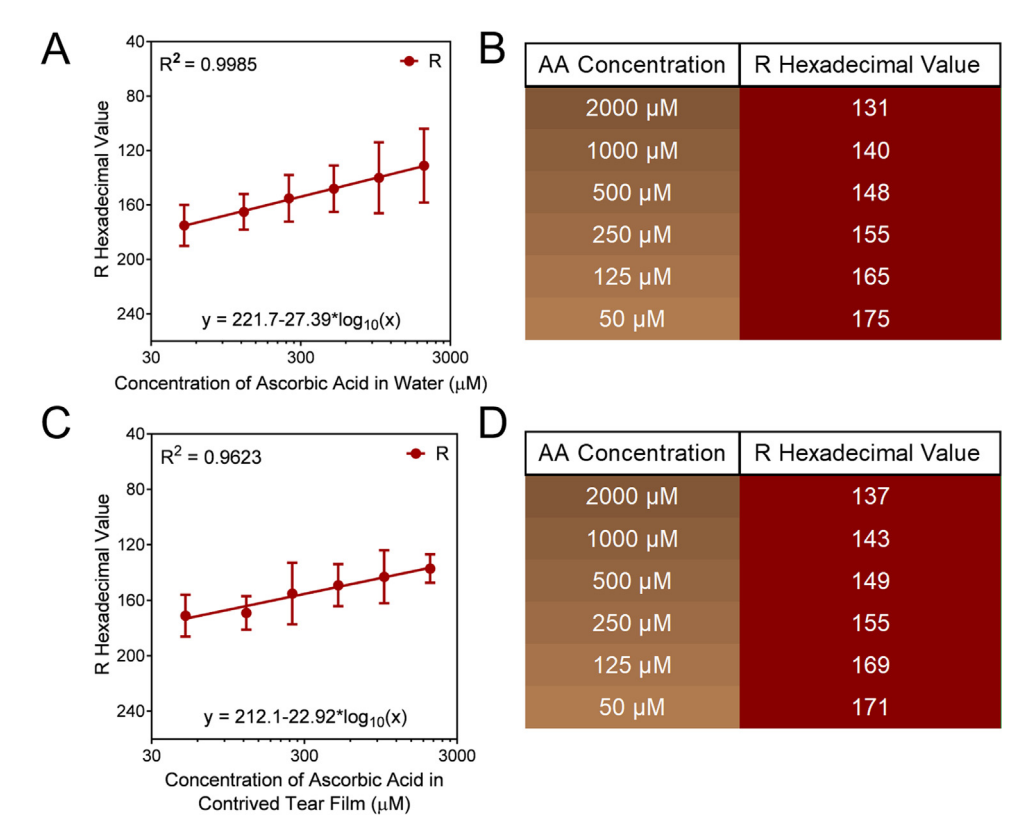


Fig. 3. Hexadecimal R values from photographed OjoGels as a function of AA concentration (50–2000 μM) in DI-H₂O (A) (n = 50 images) and (50–2000 μM) CTF (C) (n = 50 images). Hexadecimal R values from photographed OjoGels as a function of AA concentration in DI-H₂O (B) (n = 50 images) and CTF (D) (n = 50 images).

AA (1 mM; Spot 2) (Fig. 2D) and AH incubation (AH1; Spot 5) (Fig. 2E) dissolved with sodium hypochlorite solution and Raman scattering patterns (Fig. 2 F). To determine the colorimetric relationship, 50 pictures were captured of each titrated AA treatment (2000, 1000, 500, 250, 100 and 50 μ M) using a camera phone (Apple iPhone 7 (12 MP, f/ 1.8, 28 mm, 1/3", phase detection autofocus, OIS, quad-LED dual-tone flash)), and the average RGB values were numerically determined using the Pixel Picker® application (available from the Apple App StoreTM).

After finding a logarithmic colorimetric relationship between AA (dissolved in DI-H₂O) and RGB values determined with Pixel Picker*, we then aimed to find if this relationship would be maintained in more complex solutions (similar to clinical samples). To discover if this colorimetric relationship would be maintained in more complex mixtures, CTF was used in place of DI-H₂O for titrated treatments of identical AA concentrations. The contents of CTF, being similar in content to biological tear film, provided an outlet for realistic testing conditions for our OjoGel without the volume limitations and variability found in clinical samples. From these treatments with titrated amounts of AA, we found a logarithmic relationship between the R hexadecimal values of the OjoGel and the AA concentration in DI-H₂O (Fig. 3A and B) CTF samples (Fig. 3C and D).

3.3. Detection of ascorbic acid in aqueous humor and validation against ELISA

To validate OjoGel as a sensor for the detection of AA in clinically relevant settings, AH samples were clinically obtained and then tested for AA using both OjoGel and ELISA (Fig. 4A–C). AA concentration of five clinical AH samples were measured in duplicate via ELISA. The calibration of the ELISA against AA was performed in duplicate by dissolving known concentrations of AA in DI- $\rm H_2O$. The AA levels in AH samples collected from subjects # 1, 2, 3, 4 and 5 are 4.079, 2.247, 5.119, 2.792, and 14.623 nM, respectively. AH samples remaining after ELISA measurement were used to treat OjoGel sensors and for each of

these treatments 50 images with corresponding RGB values were collected. The red (R) hexadecimal value for the OjoGel treated with clinical samples had an apparent logarithmic relation to concentration of AA (as determined by ELISA). A comparison of two methods OjoGel and ELISA was done to demonstrate the accuracy (% error) based on the AA level determined in the AH samples. When we used the red (R) hexadecimal values of the OjoGel treated with clinical samples to back calculate the AA concentration using the relationships calibrated in DI-H₂O and CTF, we found a logarithmic relationship within our testing range, however, at concentrations higher than those obtained via ELISA. The two methods co-related with regression value ($R^2 = 0.8995$) and showed strong validity of the proposed OjoGel for the detection of AA concentration (Fig. 4C).

3.4. Color code rings and simultaneous calculation of AA concentration in aqueous humor (AH) samples

Prepared color rings with known AA concentration color (Fig. 5B) were decorated around the neck of OjoGel sample tubes (Fig. 5A) before capillary tubes (Fig. 5C) mediated transfer of AA samples (Fig. 5D–I) on top of OjoGel tubes. Within two min of incubation a color change was noticed on the top of the OjoGel surface. Pixel Picker* app was used to catch the color and correlated with color codes on rings present around the neck of OjoGel tubes. A range of 50–2000 μM of AA was reported in different clinical AH samples.

3.5. Specificity and sensitivity of OjoGel

In our experiments, two other major components of AH, L-lactic and sialic acid, were chosen to investigate the specificity of the OjoGel. In a typical experiment, 2000 μM AA, L-lactic and sialic acid spiked in CTF were added to the OjoGel material. It was observed that with the treatment of OjoGel with AA the color of the gel would change to a mahogany/orange-brown due to an increased localized nanoparticle

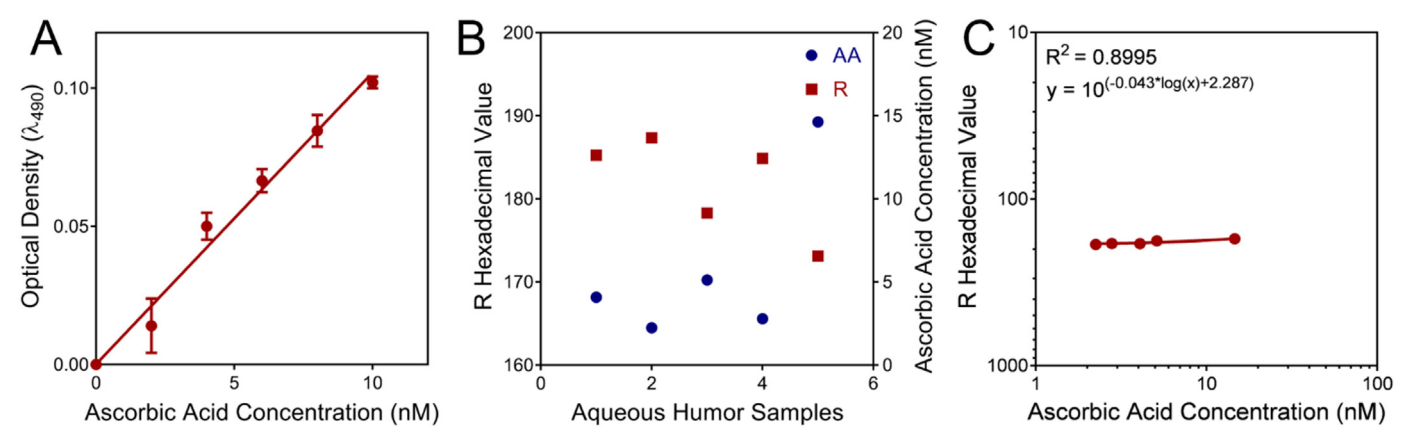


Fig. 4. (A) Concentration of AA in standard samples and correlation with absorption intensity at 490 nm. (B) Concentration of AA in clinical AH samples as calculated from Hexadecimal R values from photographed OjoGels as a function of AA concentration in water (n = 25 images). AA concentrations of 4.079, 2.247, 5.119, 2.792, and 14.623 nM are obtained in the AH samples # 1, 2, 3, 4 and 5 respectively (C) R Hexadecimal values from photographed OjoGels as a function of AA concentration in water (n = 50 images).

formation at the treatment site but remained the same when treated with CTF spiked with L-lactic acid and sialic acid (Fig. 6A). Composition of the CTF includes Potassium Chloride (KCl), Sodium Chloride (NaCl), Sodium Bicarbonate, Urea, Ammonia Chloride, Y-globulins, Vitamin C, Citric Acid, Albumins (Human), Lysozymes, Pyruvic Acid,

Lactic Acid, Hydrochloric Acid, Free Fatty Acids; Wax Esters; Cholesterol Esters; Diesters; Mucin; Free Sterols; Triglycerides; Glycerophospholipids; Sphingophospholipids; Fatty Acids and Hydrocarbons and was found to generate no significant difference in color of OjoGel due to these components. To determine this colorimetric relationship again 25

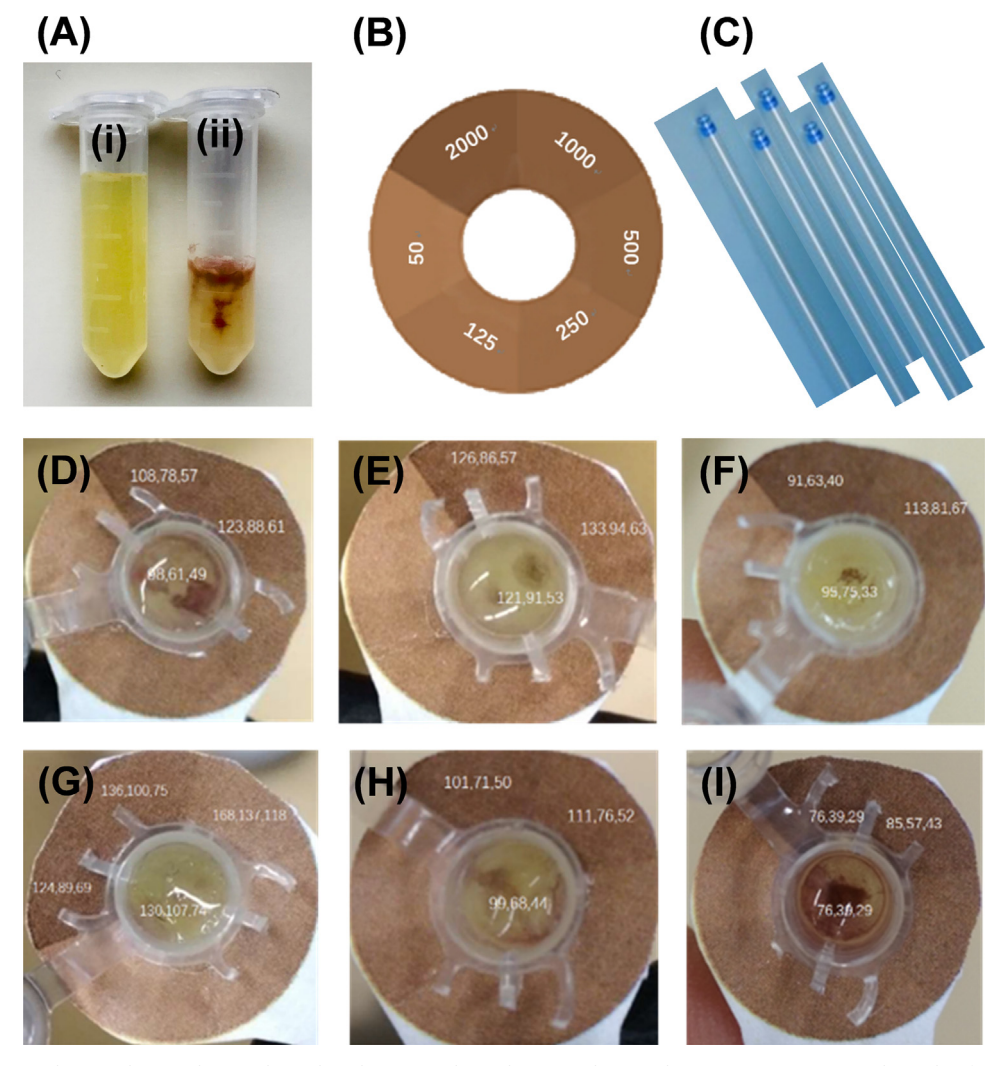


Fig. 5. (A) OjoGel tube sample (i) without and (ii) with incubated AA (B) Color code ring with printed AA concentrations, (C) glass tubes for transferring AA samples on OjoGel tubes and (D-I) AA concentrations calculated (numbers on color ring) from different AH samples calculated using Pixel Picker app.

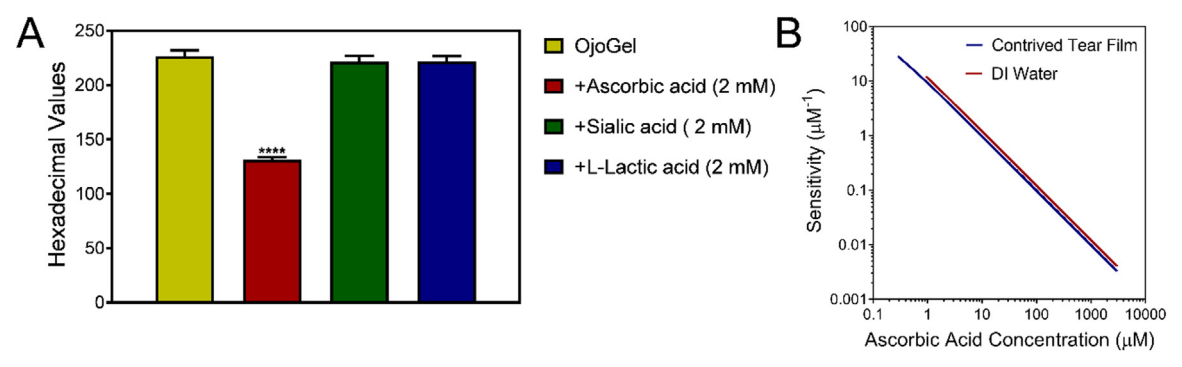


Fig. 6. (A) Specificity of OjoGel. Actual hexadecimal value of OjoGel and after treatment with L-lactic acid, Sialic acid, and Ascorbic acid. These testing confirms that ascorbic acid can be detected in tear film with high selectivity. Statistical analysis was performed using ONE WAY ANOVA comparing OjoGel background results with rest of the samples. (B) Sensitivity of AA detection in DI- H_2O and CTF samples.

pictures were captured of each titrated acid treatment using a camera phone, and the average RGB values were numerically determined using the Pixel Picker[®] application (available from the Apple App Store™). The specificity of Ojogel was found to be statistically significant over other acids and the high specificity of the OjoGel is mainly due to the high reducing activity of AA. These results manifest that AA can be detected in tear film with high selectivity. To discuss the sensitivity of the OjoGel, we must first consider that since resulting colorimetric changes are logarithmically responsive to the concentration of endogenous reductant (AA) in both pure and complex solutions (Figs. 4 and 5), that the sensitivity (RHex/[AA] (μ M⁻¹)) of these measurements will be directly dependent on the treatment concentration (Fig. 6B). This colorimetric relationship, is beneficial in that it is similarly logarithmically responsive like the human eye in perceiving light (Green, 1968; Jameson and Hurvich, 1964), in that it provides higher sensitivity between lower treatment concentrations, and that it is more able to detect lower concentrations of reductant in more complex solutions. To calculate the sensitivity (μM^{-1}) for each theoretical treatment concentrations, we took a first order derivative of the dose-response curves calibrated in DI-H2O and CTF (Fig. 3). As the relationship between sensitivity (RHex/[AA] (μ M⁻¹)) and AA concentration is inverse, we only need to calculate the detection limit to calculate the maximum sensitivity provided by our sensing material. To calculate the lowest theoretical detectable AA concentration, we would input the value of 255 = R into the logarithmic lines of best fit as calibrated in DI-H₂O and CTF. After calculating the theoretical detection limit (Table S1), we could also use this to calculate the maximum sensitivity (as described earlier). To determine the effective range of usable concentrations for our sensor, we needed to determine at what point we would consider the signal to be saturated (when the sensitivity is too low to differentiate between measurements). We arbitrarily set the saturation sensitivity as $0.2\,\mu\text{M}^{-1}$, as the Pixel Picker $^{\circ}$ phone application cannot distinguish hexadecimal values with separation less than one. Having chosen this saturation sensitivity, we could then back-calculate the concentration of AA resulting in those sensitivities for both AA in tear film and water, and then use this to calculate the saturation R value (Table S1). Furthermore, the repeatability of OjoGel was investigated by performing inter-assay variation experiment and determining the relative standard deviation (R.S.D) or coefficient of variation between different batches of OjoGel. In this regard, 9 OjoGel sensors with a same configuration were made in total three batches (27 OjoGel sensors) and treated with CTF spiked with different concentrations of AA (2000 µM, $500 \, \mu M$ and $50 \, \mu M$) to account for variability. The inter-assay R.S.D. for n = 3; samples = ((2.949 + 8.506 + 5.939)/3) = 5.798 < 10 reflects good reproducibility of results (Table S2). The repeatability of the OjoGel was investigated by performing an intra- and inter-day precision and accuracy analysis. The intra-day precision of the assay was estimated by calculating the relative standard deviation (R.S.D) for the analysis of five replicates treated with CTF spiked with different concentrations of AA (2000 μ M, 500 μ M and 50 μ M) and the inter-day precision was determined by analyzing three replicates treated with CTF spiked with different concentrations of AA (2000 μ M, 500 μ M and 50 μ M) over three consecutive days. The accuracy was calculated based on the given formula ((mean determined concentration/nominal concentration)x100). Accuracy and precision data for intra- and inter-day analysis are presented in Tables S3 and S4. The assay values on both the occasions (intra- and inter-day) were found to be within the accepted variable limits. The intra- and inter-day % accuracy values were in the range of 97.359–105.634 and 93.195–107.647 while the % precision values ranged from 3.488 to 7.288 and 5.039–8.674 respectively.

4. Conclusion

It is of great clinical significance to be able to detect the presence of a penetrating ocular injury. Unfortunately, an easy method of identifying ocular penetrating injuries is not available today. It can be difficult to identify an injury that has fully penetrated the globe even in a hospital setting. A biosensor that provides a rapid test to determine if the eye is intact to allow for appropriate triage, evacuation, and subsequent vision saving treatment can be potentially transformative. In this work we have developed a new reactive plasmonic based biosensing material composed of ionic gold interspersed through agarose gel scaffolding. Upon interaction with endogenous reductive molecules such as AA in eye fluid, the OjoGel undergoes colorimetric changes in a quantifiable manner dependent on the concentration of the reductant molecules. We have demonstrated this quantifiable colorimetric relationship with AA in solutions of varied complexity, including clinical samples. In demonstrating the capacity of the OjoGel to determine AA concentration in water, contrived tear film, and aqueous humor collected from clinical samples, we have confirmed that the OjoGel can be utilized to provide rapid quantitative detection of biologically relevant markers, like AA. With further improvement in its basic eye fluid collection device, this platform can be easily developed as a commercial product with better user supplier interface for patient care. Use of this approach may mitigate vision loss by improving the accuracy of diagnosis, and allow more efficient use of medical resources saving healthcare cost.

Acknowledgments

We thank Frederick Seitz Materials Research Laboratory Central Research Facilities, University of Illinois and Stephens Family Research Center, Carle Foundation Hospital, Children's Discovery Institute and Institute for Sustainability in Energy and Environmental Engineering and National Science Foundation for financial support. We gratefully acknowledge support from the American Heart Association (16PRE30150004).

Appendix A. Supplementary material

Supplementary data associated with this article can be found in the online version at doi:10.1016/j.bios.2018.08.019.

References

- Ajit, V., Pandya, H., 2014. TSH, PSH and GSH Comparison in Pathological Lens of Human Eye A Cataractous Study of Human, 1, pp. 138–142.
- Campbell, C.T., Kim, G., 2007. SPR microscopy and its applications to high-throughput analyses of biomolecular binding events and their kinetics. Biomaterials 28, 2380–2392. https://doi.org/10.1016/J.BIOMATERIALS.2007.01.047.
- Carrozza, C., Corsello, S.M., Paragliola, R.M., Ingraudo, F., Palumbo, S., Locantore, P., Sferrazza, A., Pontecorvi, A., Zuppi, C., 2010. Clinical accuracy of midnight salivary cortisol measured by automated electrochemiluminescence immunoassay method in Cushing's syndrome. Ann. Clin. Biochem. 47, 228–232. https://doi.org/10.1258/acb. 2010.010020.
- Choy, C.K.M., Benzie, I.F.F., Cho, P., et al., 2000. Ascorbic acid concentration and total antioxidant activity of human tear fluid measured using the FRASC assay. ... in Visassay. OphthalmolInvestig. Ophthalmol. Vis. Sci. 41 (11), 3293–3298.
- De Gelder, J., De Gussem, K., Vandenabeele, P., Moens, L., 2007. Reference database of Raman spectra of biological molecules. J. Raman Spectrosc. 38, 1133–1147. https://doi.org/10.1002/jrs.1734.
- Deng, Q., Ramsköld, D., Reinius, B., Sandberg, R., et al., 2014. Single-cell RNA-seq reveals dynamic, random monoallelic gene expression in mammalian cells. Science 343 (6167), 193–196.
- Eum, N.-S., Lee, S.-H., Lee, D.-R., Kwon, D.-K., Shin, J.-K., Kim, J.-H., Kang, S.-W., 2003. K +-ion sensing using surface plasmon resonance by NIR light source. Sens. Actuators B Chem. 96, 446–450. https://doi.org/10.1016/S0925-4005(03)00599-9.
- Evanoff, D.D., Chumanov, G., 2005. Synthesis and optical properties of silver nanoparticles and arrays. ChemPhysChem 6, 1221–1231. https://doi.org/10.1002/cphc. 200500113.
- Fredriksson, S., Gullberg, M., Jarvius, J., Olsson, C., Pietras, K., Gústafsdóttir, S.M., Östman, A., Landegren, U., 2002. Protein detection using proximity-dependent DNA ligation assays. Nat. Biotechnol. 20, 473–477. https://doi.org/10.1038/nbt0502-473.
- Green, D.G., 1968. The contrast sensitivity of the colour mechanisms of the human eye. J. Physiol. 196, 415–429. https://doi.org/10.1113/jphysiol.1968.sp008515.
- Grüb, M., Mielke, J., 2004. Aqueous humor dynamics. Ophthalmologe 101, 357–365. https://doi.org/10.1007/s00347-003-0939-3.
- Jameson, D., Hurvich, L.M., 1964. Theory of brightness and color contrast in human vision. Vis. Res. 4, 135–154. https://doi.org/10.1016/0042-6989(64)90037-9.
- Jans, H., Huo, Q., 2012. Gold nanoparticle-enabled biological and chemical detection and analysis. Chem. Soc. Rev. 41, 2849–2866. https://doi.org/10.1039/CICS15280G.
- Jeong, E.-J., Jeong, Y.S., Park, K., Yi, S.Y., Ahn, J., Chung, S.J., Kim, M., Chung, B.H., 2008. Directed immobilization of DNA-binding proteins on a cognate DNA-modified chip surface. J. Biotechnol. 135, 16–21. https://doi.org/10.1016/J.JBIOTEC.2008. 02.019
- Kattumuri, V., Chandrasekhar, M., Guha, S., Raghuraman, K., Katti, K.V., Ghosh, K., Patel, R.J., 2006. Agarose-stabilized gold nanoparticles for surface-enhanced Raman spectroscopic detection of DNA nucleosides. Appl. Phys. Lett. 88, 153114. https://doi.org/10.1063/1.2192573.
- Kaushik, A., Vasudev, A., Arya, S.K., Pasha, S.K., Bhansali, S., 2013. Recent advances in cortisol sensing technologies for point-of-care application. Biosens. Bioelectron. 53, 499–512. https://doi.org/10.1016/j.bios.2013.09.060.
- Klopfenstein, B.J., Purnell, J.Q., Brandon, D.D., Isabelle, L.M., DeBarber, A.E., 2011. Determination of cortisol production rates with contemporary liquid chromato-graphy-mass spectrometry to measure cortisol-d3 dilution after infusion of deuterated tracer. Clin. Biochem. 44, 430–434. https://doi.org/10.1016/J.CLINBIOCHEM.
- Lee, J., Ahmed, S.R., Oh, S., Kim, J., Suzuki, T., Parmar, K., Park, S.S., Lee, J., Park, E.Y., 2015. A plasmon-assisted fluoro-immunoassay using gold nanoparticle-decorated carbon nanotubes for monitoring the influenza virus. Biosens. Bioelectron. 64, 311–317. https://doi.org/10.1016/J.BIOS.2014.09.021.
- Leite, M.T., Prata, T.S., Kera, C.Z., Miranda, D.V., de Moraes Barros, S.B., Melo, L.A., 2009. Ascorbic acid concentration is reduced in the secondary aqueous humour of glaucomatous patients. Clin. Exp. Ophthalmol. 37, 402–406. https://doi.org/10. 1111/j.1442-9071.2009.02046.x.
- Luppa, M., Sikorski, C., Luck, T., Weyerer, S., Villringer, A., König, H.-H., Riedel-Heller, S.G., 2012. Prevalence and risk factors of depressive symptoms in latest life-results of the Leipzig longitudinal study of the aged (LEILA 75+). Int. J. Geriatr. Psychiatry 27, 286–295. https://doi.org/10.1002/gps.2718.
- Manenschijn, L., Koper, J.W., Lamberts, S.W.J., van Rossum, E.F.C., 2011. Evaluation of a method to measure long term cortisol levels. Steroids 76, 1032–1036. https://doi. org/10.1016/J.STEROIDS.2011.04.005.

- Matsui, T., Kitagawa, Y., Okumura, M., Shigeta, Y., 2015. Accurate standard hydrogen electrode potential and applications to the redox potentials of vitamin C and NAD/ NADH. J. Phys. Chem. A 119, 369–376. https://doi.org/10.1021/jp508308y.
- Millar, J.C., Phan, T.N., Pang, I.-H., 2018. Assessment of Aqueous Humor Dynamics in the Rodent by Constant Flow Infusion. Humana Press, New York, NY, pp. 109–120. https://doi.org/10.1007/978-1-4939-7407-8_11.
- Nie, M., Xie, Y., Loo, J.A., Courey, A.J., 2009. Genetic and proteomic evidence for roles of drosophila SUMO in cell cycle control, Ras signaling, and early pattern formation. PLoS One 4, e5905. https://doi.org/10.1371/journal.pone.0005905.
- Patskovsky, S., Jacquemart, R., Meunier, M., De Crescenzo, G., Kabashin, A.V., 2008. Phase-sensitive spatially-modulated surface plasmon resonance polarimetry for detection of biomolecular interactions. Sens. Actuators B Chem. 133, 628–631. https://doi.org/10.1016/J.SNB.2008.03.044.
- Qin, Y., Ji, X., Jing, J., Liu, H., Wu, H., Yang, W., 2010. Size control over spherical silver nanoparticles by ascorbic acid reduction. Colloids Surf. A Physicochem. Eng. Asp. 372, 172–176. https://doi.org/10.1016/J.COLSURFA.2010.10.013.
- Qiu, Guangyu, Ng, Siu Pang, Wu, Chi-Man Lawrence, 2018. Label-free surface plasmon resonance biosensing with titanium nitride thin film. Biosensors and Bioelectronics 106, 129–135. https://doi.org/10.1016/j.bios.2018.02.006.
- Sannomiya, T., Hafner, C., Voros, J., 2008. In situ sensing of single binding events by localized surface plasmon resonance. Nano Lett. 8, 3450–3455. https://doi.org/10. 1021/nl802317d.
- Schuller, J.A., Barnard, E.S., Cai, W., Jun, Y.C., White, J.S., Brongersma, M.L., 2010. Plasmonics for extreme light concentration and manipulation. Nat. Mater. 9, 193–204. https://doi.org/10.1038/nmat2630.
- Schwartz-Duval, A.S., Misra, S.K., Mukherjee, P., Johnson, E., Acerbo, A.S., Pan, D., 2016. An anisotropic propagation technique for synthesizing hyperbranched polyvillic gold nanoparticles. Nano Res. 9, 2889–2903. https://doi.org/10.1007/s12274-016-1174-y.
- Shankaran, D.R., Gobi, K.V., Miura, N., 2007. Recent advancements in surface plasmon resonance immunosensors for detection of small molecules of biomedical, food and environmental interest. Sens. Actuators B Chem. 121, 158–177. https://doi.org/10. 1016/J.SNB.2006.09.014.
- Song, F., Parekh, S., Hooper, L., Loke, Y., Ryder, J., Sutton, A., Hing, C., Kwok, C., Pang, C., Harvey, I., 2010. Dissemination and publication of research findings: an updated review of related biases. Health Technol. Assess. (Rockv.) 14, 1–193. https://doi.org/10.3310/hta14080.
- Sotiriou, G.A., Sannomiya, T., Teleki, A., Krumeich, F., Vörös, J., Pratsinis, S.E., 2010. Non-toxic dry-coated nanosilver for plasmonic biosensors. Adv. Funct. Mater. 20, 4250–4257. https://doi.org/10.1002/adfm.201000985.
- Takemura, K., Adegoke, O., Takahashi, N., Kato, T., Li, T.-C., Kitamoto, N., Tanaka, T., Suzuki, T., Park, E.Y., 2017. Versatility of a localized surface plasmon resonance-based gold nanoparticle-alloyed quantum dot nanobiosensor for immunofluorescence detection of viruses. Biosens. Bioelectron. 89, 998–1005. https://doi.org/10.1016/J.BIOS.2016.10.045.
- Taylor, A., Jacques, P.F., Epstein, E.M., 1995. Relations among aging, antioxidant status, and cataract. Am. J. Clin. Nutr. 62, 14398–1447S. https://doi.org/10.1093/ajcn/62.
- Tian, Y., Tatsuma, T., 2005. Mechanisms and applications of plasmon-induced charge separation at TiO2 films loaded with gold nanoparticles. J. Am. Chem. Soc. 127, 7632–7637. https://doi.org/10.1021/ja042192u.
- Uechi, I., Yamada, S., 2008. Photochemical and analytical applications of gold nanoparticles and nanorods utilizing surface plasmon resonance. Anal. Bioanal. Chem. 391, 2411–2421. https://doi.org/10.1007/s00216-008-2121-x.
- Vallejo-Illarramendi, A., Marciano, D.K., Reichardt, L.F., 2013. A novel method that improves sensitivity of protein detection in PAGE and Western blot. Electrophoresis 34, 1148–1150. https://doi.org/10.1002/elps.201200534.
- Vo-Dinh, T., Cullum, B., 2000. Biosensors and biochips: advances in biological and medical diagnostics. Fresenius J. Anal. Chem. 366, 540–551. https://doi.org/10. 1007/s002160051549.
- Wang, T., Wei, J.J., Sabatini, D.M., Lander, E.S., et al., 2014. Genetic screens in human cells using the CRISPR-Cas9 system. Science 343 (6166), 80–84.
- Whitcombe, M.J., Chianella, I., Larcombe, L., Piletsky, S.A., Noble, J., Porter, R., Horgan, A., 2011. The rational development of molecularly imprinted polymer-based sensors for protein detection. Chem. Soc. Rev. 40, 1547–1571. https://doi.org/10.1039/COCS00049C.
- Willets, Katherine A, Van Duyne, Richard P, 2007. Localized Surface Plasmon Resonance Spectroscopy and Sensing. Annu. Rev. Phys. Chem 58 (1), 267–297.
- Yeom, S.-H., Han, M.-E., Kang, B.-H., Kim, K.-J., Yuan, H., Eum, N.-S., Kang, S.-W., 2013. Enhancement of the sensitivity of LSPR-based CRP immunosensors by Au nanoparticle antibody conjugation. Sens. Actuators B Chem. 177, 376–383. https://doi. org/10.1016/J.SNB.2012.10.099.
- Yuan, H., Khoury, C.G., Hwang, H., Wilson, C.M., Grant, G.A., Vo-Dinh, T., 2012. Gold nanostars: surfactant-free synthesis, 3D modelling, and two-photon photoluminescence imaging. Nanotechnology 23, 75102. https://doi.org/10.1088/0957-4484/23/7/075102.